

Comparison of Perturbative RG Theory with Lattice Data for the $4d$ Ising Model

P. M. Stevenson

T. W. Bonner Laboratory, Department of Physics and Astronomy
Rice University, P.O. Box 1892, Houston, TX 77251-1892, USA

Abstract:

Predictions for $(\phi^4)_4$ theory from renormalization-group-improved perturbation theory, as formulated by Lüscher and Weisz, are compared to published (and some unpublished) data from lattice Monte-Carlo simulations of the 4-dimensional Ising model. Good agreement is found in all but one respect:— the change in the wavefunction-renormalization constant \hat{Z}_R across the phase transition is significantly greater than predicted. A related observation is that propagator data in the broken phase show deviations from free-propagator form — deviations that become larger, not smaller, closer to the continuum limit. More data closer to the critical point are needed to clarify the situation.

1 Introduction

A complete understanding of the $(\phi^4)_4$ theory is important not only as a fundamental problem in quantum field theory, but also for its implications for the Higgs mechanism. According to conventional wisdom the continuum limit of lattice $(\phi^4)_4$ theory is described by a Renormalization Group (RG) analysis using RG functions calculated in perturbation theory. The theory was developed in detail by Brézin *et al* [1] and by Lüscher and Weisz (LW) [2, 3]. It predicts “triviality” in the sense that the renormalized coupling g_R tends to zero.

In the late eighties LW’s numerical predictions were compared with Monte-Carlo data for the 4-dimensional Ising model in both the symmetric phase [4, 5] and the broken phase [6]. The aim of this paper is to revisit this comparison in the light of the much larger data set now available [7, 8, 9, 10].

One motivation for this exercise is the recent controversy between Balog, Duncan, Willey, Niedermayer and Weisz (BDWNW) [8] and Cea, Consoli, and Cosmai (CCC) [7]. It is important to note that the raw data of the two groups agree very well; the dispute is solely over interpretation. I cannot pretend that my sympathies are neutral; for many years I have collaborated closely with CCC in gathering lattice Monte-Carlo evidence [9, 11] for an unconventional view of “triviality” in $(\phi^4)_4$ theory advocated by Consoli and myself [12]. Nevertheless, I intend here to take a detached view and, except for a few remarks in Sect. 5, I shall not discuss the ideas of Ref. [12]. No change in my position is implied; I simply want to focus here on a limited question: *how well does perturbative RG theory agree with all the available lattice data?*

While BDWNW and CCC both describe fits of their data to formulas based on 1- or 2-loop perturbation theory, neither group has made a comprehensive comparison to the full LW theory incorporating 3-loop and higher-twist effects. That exercise is performed here in Sect. 3, considering all measured quantities in the both the broken and symmetric phases. Good agreement is found, except for the wavefunction-renormalization constant \hat{Z}_R , as discussed in Sect. 4. Broken-phase propagator data are examined in Sect. 5. BDWNW’s data show the same deviation from free-propagator behaviour found in Ref. [9]. Because of this deviation, different strategies for extracting “mass” and “ \hat{Z} ” parameters can lead to very different conclusions. Non-Ising data are briefly considered in Sect. 6 and conclusions are summarized in Sect. 7. An appendix gives a detailed discussion of the data used.

2 Basic definitions

I shall use the notation of LW and BDWNW and I refer the reader to those papers for full definitions. Only a few key facts will be outlined here. The lattice action for the ϕ^4 theory is written as

$$S = \sum_x \left[-2\kappa \sum_{\mu=1}^4 \phi(x)\phi(x + \hat{\mu}) + \phi(x)^2 + \lambda (\phi(x)^2 - 1)^2 \right], \quad (1)$$

which is equivalent to the more traditional expression

$$S = \sum_x \left[\frac{1}{2} \sum_{\mu=1}^4 (\partial_\mu \phi_0(x))^2 + \frac{1}{2} m_0^2 \phi_0(x)^2 + \frac{g_0}{4!} \phi_0^4 \right], \quad (2)$$

where $\partial_\mu \phi_0(x) = \phi_0(x + \hat{\mu}) - \phi_0(x)$. The translation between the two formulations is given by

$$\phi_0 = \sqrt{2\kappa} \phi, \quad m_0^2 = \frac{(1 - 2\lambda)}{\kappa} - 8, \quad g_0 = \frac{6\lambda}{\kappa^2}. \quad (3)$$

LW also define another parameter $\bar{\lambda}$ that varies between 0 and 1 as λ ranges from 0 to ∞ . The limit $\lambda \rightarrow \infty$ ($\bar{\lambda} = 1$) corresponds to the Ising model, where $\phi(x)$ can take only the values ± 1 . For a given $\bar{\lambda}$ there is a critical κ separating the symmetric and broken phases. As $\kappa \rightarrow \kappa_c$ the correlation length (inverse of the physical mass in lattice units) diverges, according to the RG theory, so that $\kappa \rightarrow \kappa_c$ corresponds to the continuum limit.

The $\sqrt{2\kappa}$ factor between the Ising field ϕ and the canonical field ϕ_0 is the source of several notational nuisances. In particular, the field renormalization constant Z_R defined by LW includes both the trivial 2κ factor and the dynamical effects. I follow BDWNW in defining $\hat{Z}_R = 2\kappa Z_R$ as the canonical field renormalization that obeys $\hat{Z}_R < 1$. The renormalized coupling constant g_R and renormalized mass m_R are defined as in LW, as are the susceptibility χ and vacuum expectation value $v = \langle \phi \rangle$. To plot the data for the latter quantities I have first removed the power-law dependence on $(\kappa - \kappa_c)$ by defining

$$\tilde{\chi} \equiv \chi(\kappa - \kappa_c), \quad \tilde{v}^2 = v^2/(\kappa - \kappa_c). \quad (4)$$

Notice that the combination χv^2 is “dimensionless” in this sense.

The RG theory involves coupled differential equations containing three RG functions β , γ and δ . LW provide a recipe for constructing these functions to 3-loop

order, including power-suppressed (or “higher twist”) scaling violations to 1-loop order. The higher-twist terms, while negligible in the limit $\kappa \rightarrow \kappa_c$, are important further away from κ_c . Because of them the integration of the differential equations must be done numerically. Using *Mathematica*, I have implemented LW’s procedure exactly as described in Refs. [2], [3] (referred to below as LW(I) and LW(II), respectively).¹ The LW procedure depends upon three integration constants C_1, C_2, C_3 as well as on the assumed value for κ_c . I have verified that my program precisely reproduces the results in the LW tables when the same input parameters are used. (The C_i constants are defined in the symmetric phase; in the broken phase LW define corresponding constants C'_1, C'_2, C'_3 and then prove that $C'_1 = e^{1/6}C_1$, while $C'_2 = C_2$ and $C'_3 = C_3$. I shall quote only numerical values for the C'_i ’s, but of course the conversion from C_1 to C'_1 is taken into account in my program.)

In the Ising case a quite precise value for κ_c is known [13]:

$$\kappa_c = 0.074848(2) \tag{5}$$

and will be adopted here. This value is consistent with earlier estimates, 0.074834(15) [14] and 0.074851(8) [15]. [In fact, I initially made fits using 0.074834 and then tried 0.074851 and found a small but distinct improvement. On closer inspection, the improvement seemed to have slightly “overshot” and I was experimenting with slightly smaller “compromise” values when I became aware of the result of Ref. [13]. Thus, I adopt that value both because it has the smallest quoted uncertainty and because it seems to produce the best fits.]

3 Fits to lattice data

Table 1 of LW(II) gives predictions for the three integration constants based on LW(I)’s analysis that matched the RG procedure to the “high-temperature” (small κ) expansion in the symmetric phase. For the Ising model these predictions are

$$\ln C_1 = 1.5(2), \quad \ln C_2 = 1.87(1), \quad \ln C_3 = -3.0(1). \tag{6}$$

One can indeed fit the available symmetric-phase data quite well with parameters in this range (see later). However, these parameter values do not yield a good fit to the broken-phase data. This observation is in accord with the experience of CCC [7].

¹Copies of my *Mathematica* programs are available upon request.

However, BDWNW [8] point out that, with hindsight, the uncertainties quoted by LW may have been over-optimistically small, especially in the Ising case. Also, LW used a much cruder approximate value for κ_c (0.07475(7)) which is another source of the discrepancies found by CCC. By adjusting the values of κ_c and the C_i 's, BDWNW claim one can fit the broken-phase data very well with the conventional RG theory. To check this assertion, I have considered all available Monte-Carlo Ising data (see Appendix) and made a number of fits, adjusting the parameters by trial and error. Fig. 1 shows the best fit I have obtained, which uses the following parameter values:

$$\ln C_1 = 1.24, \quad \ln C_2 = 1.83, \quad \ln C_3 = -2.90. \quad (7)$$

Indeed, this fit seems to be an entirely satisfactory description of the broken-phase data, given the theoretical uncertainties, especially at the larger κ 's.

Comparing these parameter values with the LW values quoted above one sees a lower $\ln C_1$ value – in accord with a remark in BDWNW that a value ~ 1.2 is needed. However, note also the lower $\ln C_2$ value, which will be crucial in what follows.

[It is hard to quote meaningful uncertainties on the “best fit” parameter values given above. The effects of varying the C_i 's are highly correlated, difficult to describe, and often hard to understand intuitively. Also, one should give more weight to fitting the data points closer to κ_c , where the theoretical uncertainties are less. As a very rough guide I would say that changing any of the $\ln C_i$ values in Eq. (7) by plus or minus 0.06, 0.01, 0.01, respectively, would lead to a discernible deterioration in the quality of the fit and changes by twice these amounts would be unacceptable.]

However, while the C_i values in Eq. (7) yield an excellent fit to the broken-phase data, they do *not* yield a good fit to the symmetric-phase data; see Fig. 2. The fits to m_R and g_R are quite good, but the theoretical curve for \hat{Z}_R lies far below the data points. That fact is a direct consequence of the lower C_2 value, since \hat{Z}_R has a factor of C_2 .

If one increases $\ln C_2$ to 1.862 (back in accord with LW's predicted value) one can then obtain a good fit to symmetric phase data; see Fig. 3. However, this change spoils the fit to the broken-phase data, not only for \hat{Z}_R , but also for $\tilde{\chi}$ and \tilde{v} ; see Fig. 4. I have tried adjusting the C_i 's further but I cannot find any “compromise” values that would make the problem go away. One can fit either the broken-phase data, or the symmetric-phase data — but one cannot fit both well simultaneously.

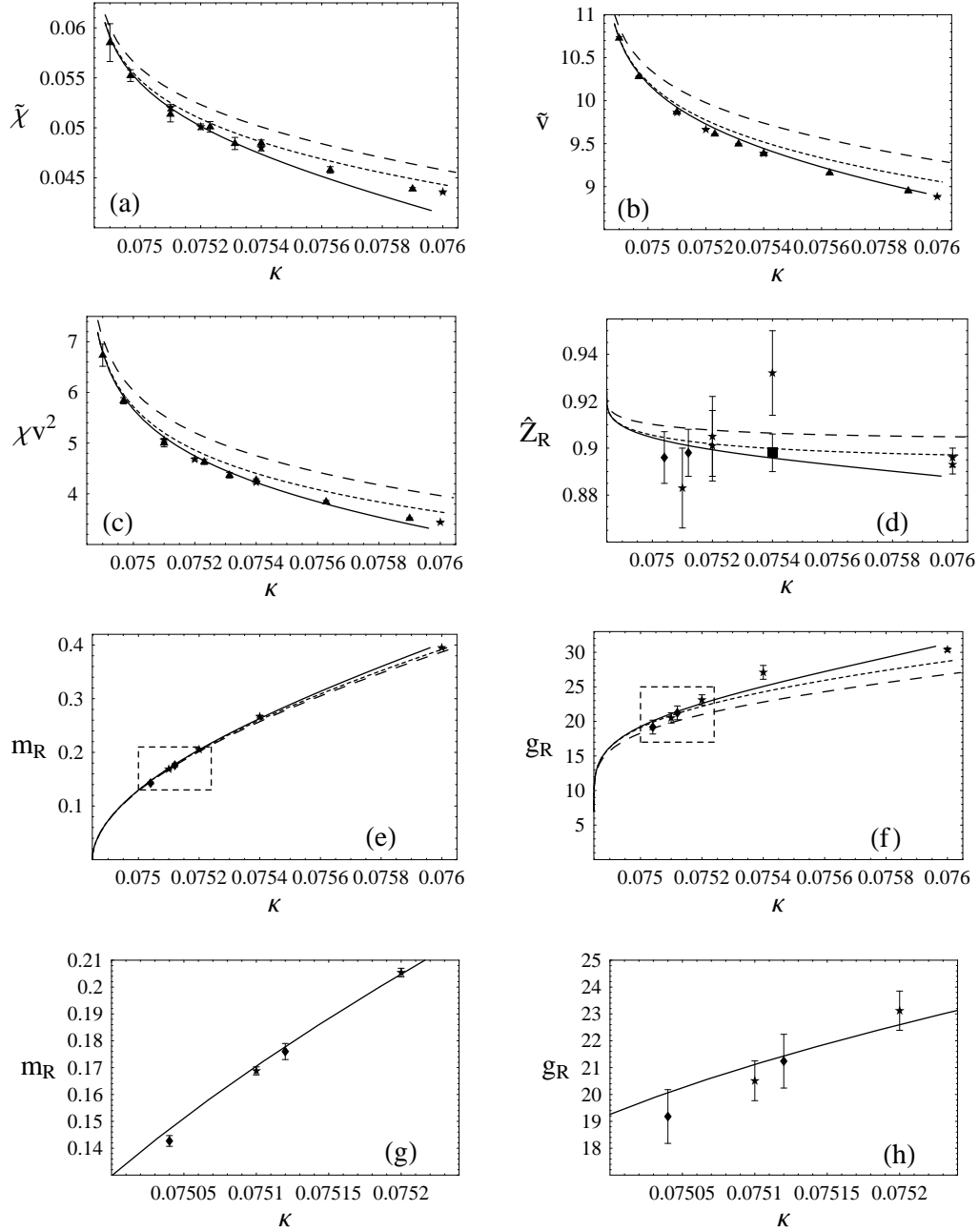


Figure 1: Broken-phase data for the Ising model compared with the LW procedure for parameters $\ln C_1 = 1.24$, $\ln C_2 = 1.83$, $\ln C_3 = -2.90$, and $\kappa_c = 0.074848$. The solid curve is the full LW procedure (3-loops plus higher-twist corrections to 1-loop). The long-dashed lines show the effect of omitting 3-loop terms, while the short-dashed lines show the effect of omitting higher-twist terms. The boxed regions in (e) and (f) are shown on an expanded scale in (g) and (h). Data points from Refs. [6, 7, 8, 9, 10], see Appendix for details.

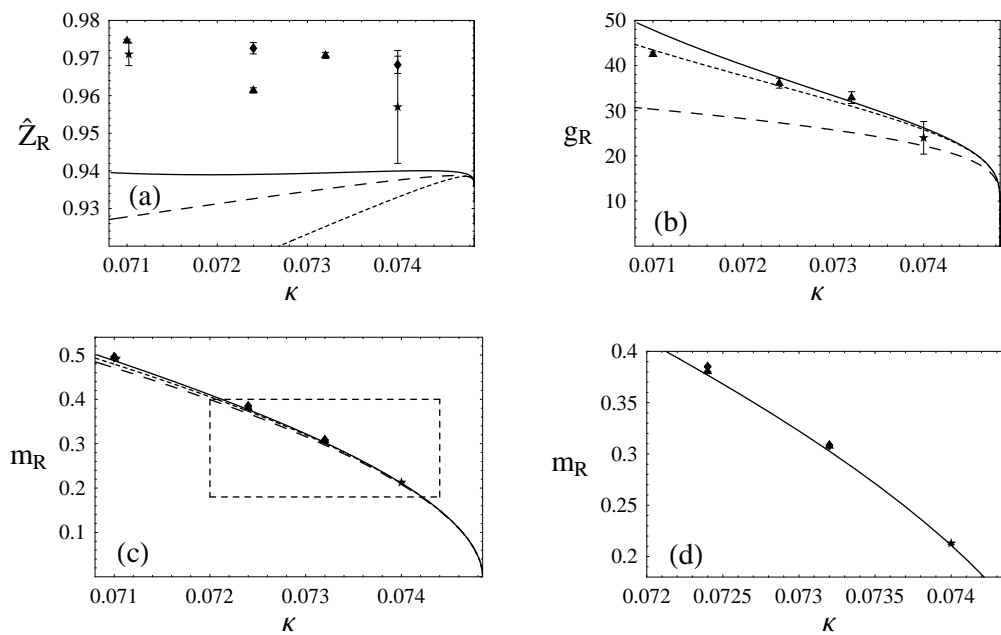


Figure 2: Symmetric-phase data for the Ising model compared with the LW procedure for the same parameters as Fig. 1. Note that in (a) the curve lies well below the \hat{Z}_R data points. The boxed region in (c) is shown in more detail in (d). Data points from Refs. [4, 5, 9, 10], see Appendix.

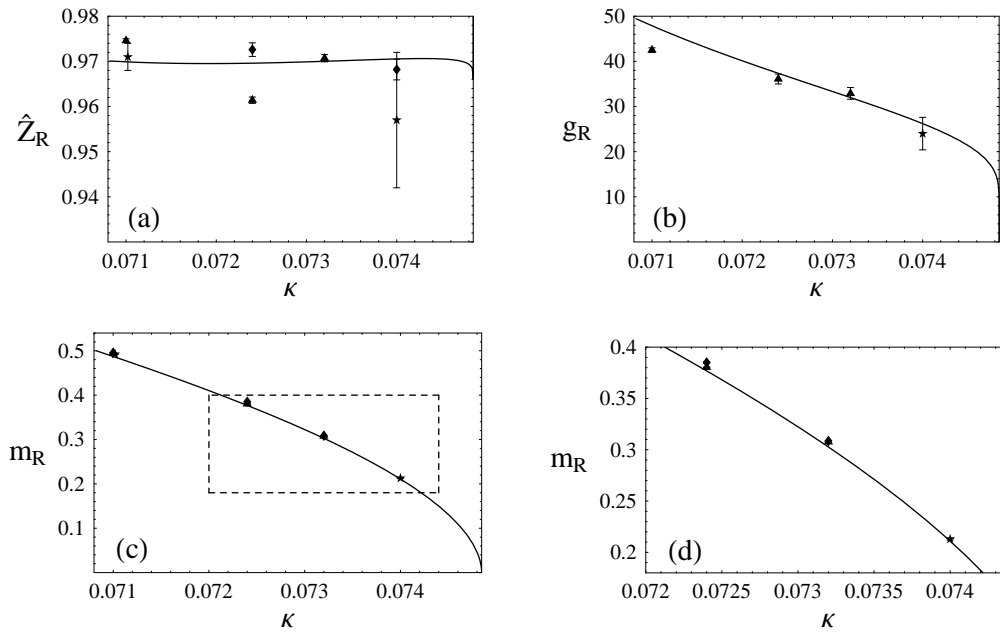


Figure 3: As Fig. 2 but with $\ln C_2$ increased to 1.862 so as to obtain a good fit to the symmetric-phase \hat{Z}_R data.

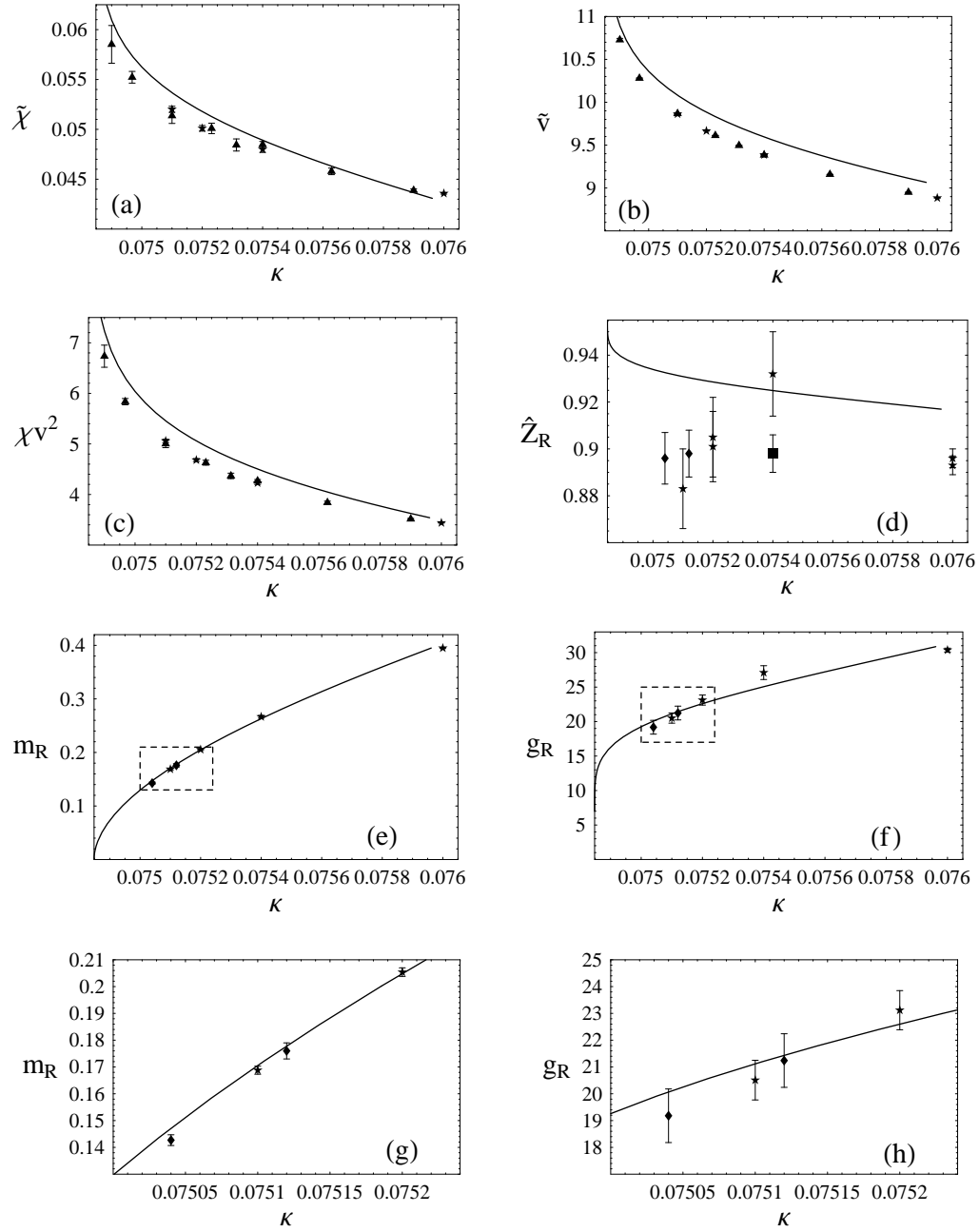


Figure 4: Fits to the broken-phase data with the same parameters as in Fig. 3: $\ln C_1 = 1.24$, $\ln C_2 = 1.862$, $\ln C_3 = -2.90$. Note that these parameters are basically in accord with LW's predicted values, Eq. (6). Compared to Fig. 1 the fits to $\tilde{\chi}$, \tilde{v} , χv^2 , as well as \hat{Z}_R in (a)–(d) are spoiled, though there is little or no effect on (e)–(h).

4 The “step” in \hat{Z}_R

The essence of the problem is illustrated in Figure 5, which shows \hat{Z}_R on *both* sides of the phase transition, combining Figs 2(a) and 1(d) on a common scale. It is convenient to define the “step” as:

$$\Delta = \hat{Z}_R(\kappa=0.074) - \hat{Z}_R(\kappa=0.0751). \quad (8)$$

From the CCCS data point at 0.074 and combining the five data points around 0.0751 one finds an “experimental” value of $\Delta = 0.071(6)$. However, the theoretical curve predicts a step of only about 0.04. Moreover, as argued below, this is a robust prediction, essentially independent of the particular C_i values, and with little theoretical uncertainty.

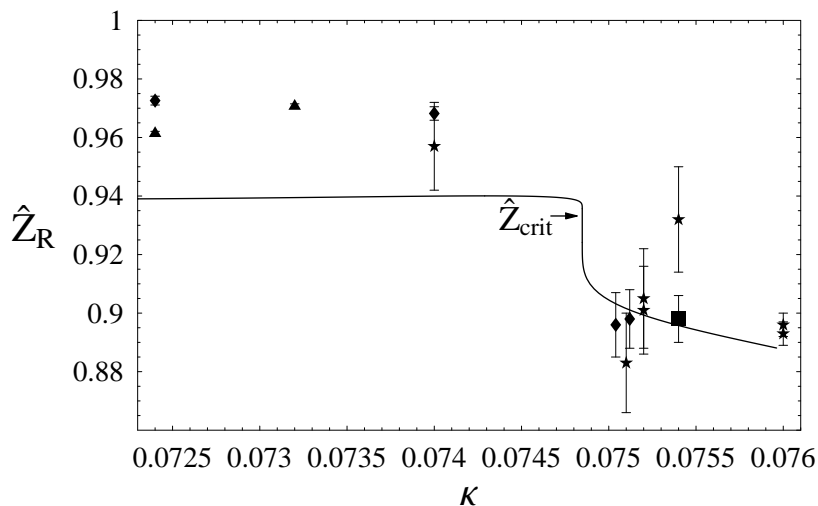


Figure 5: The “step” in \hat{Z}_R across the phase transition. The data indicate a step of 0.07, whereas the predicted step is only 0.04. The solid curve is for the parameters of Eq. (7) used in Figs. 1 and 2. Increasing C_2 and hence $\hat{Z}_{\text{crit}} \equiv 2\kappa_c C_2$ would shift the theoretical curve upward with almost no change in shape. See also Fig. 12.

The theoretical prediction for \hat{Z}_R can be understood simply if we neglect higher-twist effects. In the symmetric phase it takes the form

$$\hat{Z}_R = \hat{Z}_{\text{crit}} \left(\frac{2\kappa}{2\kappa_c} \right) \left(1 + \frac{1}{18}\alpha + 0.100896\alpha^2 + \dots \right), \quad (9)$$

where

$$\hat{Z}_{\text{crit}} \equiv 2\kappa_c C_2 \quad \text{and} \quad \alpha = g_R/(16\pi^2). \quad (10)$$

At $\kappa = 0.074$, the measured g_R is about 27, so $\alpha = 0.171$ and the series is well-behaved. Numerically one finds, adding on a higher-twist contribution based on the fit in Fig. 2:

$$\hat{Z}_R(\kappa=0.074) = \hat{Z}_{\text{crit}}(0.9887)(1.0124) + 0.0080. \quad (11)$$

[Note that in Fig. 2(a) the higher-twist contribution is quite sizeable. Curiously, it seems to compensate for the linear rise caused by the κ/κ_c factor, so that \hat{Z}_R is almost flat until very close to κ_c .] In the broken phase one has

$$\hat{Z}_R = \hat{Z}_{\text{crit}} \left(\frac{2\kappa}{2\kappa_c} \right) \left(1 - \frac{7}{36}\alpha - 0.538874\alpha^2 + \dots \right). \quad (12)$$

At $\kappa = 0.0751$ the measured g_R is about 21, so $\alpha = 0.133$ and again the series is well behaved. Numerically, adding on a higher-twist contribution, one obtains

$$\hat{Z}_R(\kappa=0.0751) = \hat{Z}_{\text{crit}}(1.0034)(0.9646) - 0.0017. \quad (13)$$

Hence, the numerical prediction for Δ is

$$\Delta = 0.0331\hat{Z}_{\text{crit}} + 0.0097. \quad (14)$$

The broken-phase data suggest $\hat{Z}_{\text{crit}} \approx 0.933$ while the symmetric-phase data imply 0.963; in any case, \hat{Z}_{crit} is certainly less than 1. The higher-twist contribution depends in principle on the C_i parameters, but seems to vary little in the various fits I have made. There may be some further correction from higher-loop higher-twist contributions, but these should be only a fraction of the higher-twist contribution already allowed for. Thus, the theoretical prediction for Δ cannot really be pushed above 0.05, well short of the “experimental” value 0.071(6).

This is not an entirely new problem. It was noted by Jansen *et al* [6] that there was a “small discrepancy” for \hat{Z}_R ; their data point at $\kappa = 0.076$ was about 2.5σ below the LW prediction. (That is indeed what we see in Fig. 4(d) above.) The same problem showed up in Ref. [16]. At that time it was not unreasonable to suppose that higher-order/higher-twist effects could explain away the discrepancy. However, now that there is data much closer to κ_c that explanation is no longer very credible.

5 Propagator data

Another indication that something unconventional may be going on comes from data for the momentum-space propagator. Ref. [9], referred to as CCCS below,

found that the propagator in the broken phase shows significant deviations from free-propagator form. Moreover, those deviations become *more* evident closer to κ_c , contrary to conventional ideas about “triviality.” In this section I re-examine that data and also point out that BDWNW’s data show the same effect.

Some technical preliminaries are needed. $G(\hat{p}^2)$ is defined as the Fourier transform of the connected two-point function. I shall normalize to the *canonical* field ϕ_0 ; hence my G differs by a 2κ factor from BDWNW, but agrees with CCCS. On an L^4 lattice the allowed momenta are $p_\mu = \frac{2\pi}{L}n_\mu$, where n_μ is a vector with integer-valued components and the variable \hat{p}^2 , the lattice analogue of the invariant $p^\mu p_\mu$, is defined as $4\sin^2(p_\mu/2)$, summed over $\mu = 0, \dots, 4$.

BDWNW do not directly provide propagator data in the Ising case (though they do in two non-Ising cases; see the next section). However, their Table 2 gives data for the time-slice correlation function $S(t)$ at $\kappa = 0.0751$ on a 48^4 lattice. From this data one can construct the momentum-space propagator $G(\hat{p}^2)$ for momenta $p = (2\pi/48)n$ ($n = 0, 1, 2, \dots$) along the time axis by taking the Fourier transform:

$$\frac{G(\hat{p}^2)}{2\kappa} = \sum_{t=0}^{47} S(t)e^{ipt} = S(0) + 2 \sum_{t=1}^{23} S(t) \cos pt + (-1)^n S(24).$$

(The property $S(t) = S(48 - t)$ has been used. The 2κ factor is to convert to the canonical normalization.) Without access to the raw data, I am not able to compute realistic error bars, but the smoothness of the data, and the good agreement with CCCS’s data, both suggest that the error bars would be comparable to those of CCCS.

The resulting $G(\hat{p}^2)$ points are plotted in Figure 6 in various ways. BDWNW’s remark, at the end of Sect. 5, that “the inverse propagator is remarkably linear in \hat{k}^2 up to the maximal (on-axis) momentum $\hat{k}^2 = 4$ ” is seemingly justified by Fig. 6(b). However, the parameters for this linear fit are quite different from those that BDWNW obtained from the low-momentum points (see Fig. 6(a)).

Deviations from free-propagator behaviour are more easily seen by plotting the quantity

$$\zeta = \zeta(\hat{p}^2, m) \equiv G(\hat{p}^2)(\hat{p}^2 + m^2). \quad (15)$$

Of course, ζ depends crucially on what one chooses to use as the “mass,” m . Fig. 6(c) uses the $m_R = 0.1691$ value given by BDWNW in Table 5, while Fig. 6(d) uses the larger mass, 0.200, of the fit line in Fig. 6(b) and shows a ζ that is remarkably

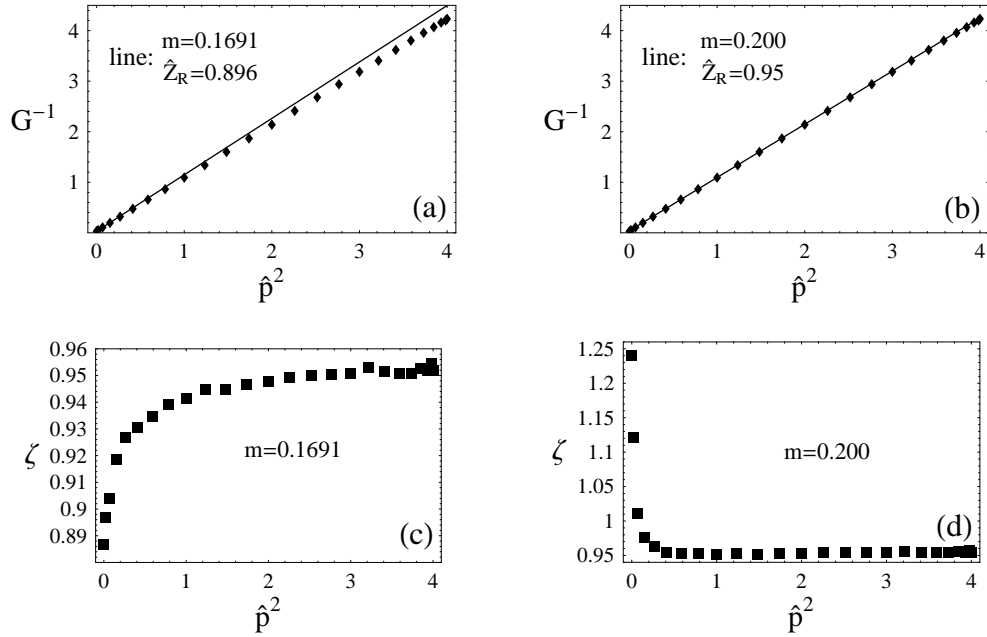


Figure 6: Propagator data for $\kappa = 0.0751$ from BDWNW plotted in various ways. No error bars are shown. (a) shows the inverse propagator G^{-1} with the straight line being BDWNW's free-propagator fit to the first three $p \neq 0$ points (see Table 5 of Ref. [8]). (b) shows another straight-line fit to the same data that is good at almost all momenta. However, the line actually fails to fit the lowest momentum points. (c) and (d) show the corresponding ζ plots, $\zeta \equiv G(\hat{p}^2)(\hat{p}^2 + m^2)$, in which the deviations from free-propagator behaviour are more easily seen.

constant except for a dramatic spike at low momentum — just as seen in Figs. 3, 4, 5 of CCCS [9].

It is necessary to distinguish three different “masses.” From the conventional viewpoint, the physical mass is determined from the exponential fall-off in time of the time-slice correlator for zero 3-momentum, $S(t)$. I denote this mass by $m_{TS}(0)$, as in CCCS. The measured values of $m_{TS}(0)$ from CCCS are shown in the second column of Table 1.

In the LW procedure the “renormalized mass” m_R and the wavefunction renormalization constant \hat{Z}_R are defined in terms of an expansion of the inverse propagator about $\hat{p}^2 = 0$:

$$G(\hat{p}^2)^{-1} = \hat{Z}_R^{-1} (m_R^2 + \hat{p}^2 + O(\hat{p}^4)). \quad (16)$$

This means that $\zeta(\hat{p}^2, m_R)$, plotted against \hat{p}^2 , should have zero slope at the origin. I have used this fact to determine m_R empirically for the CCCS data sets at $\kappa = 0.076, 0.07512, 0.07504$, adjusting m until the lowest \hat{p}^2 points lined up. (See Figs. 7, 8, 9.) The resulting m_R values, given in the third column of Table 1, are only slightly larger than the $m_{TS}(0)$ values. The ratio between the two is quite consistent with the theoretically predicted formula [3, 6]. For most of the subsequent discussion the small difference between $m_{TS}(0)$ and m_R can be ignored.

The third “mass,” denoted by m_{latt} , corresponds, as in Figs. 6(b,d), to the mass that gives the best fit to a free-propagator form:

$$G(\hat{p}^2)^{-1} \simeq \hat{Z}_{\text{prop}}^{-1} (\hat{p}^2 + m_{\text{latt}}^2), \quad (17)$$

at all momenta, excepting the first few low-momentum points. The values found by CCCS are given in the last column of Table 1.

κ	$m_{TS}(0)$	m_R	m_{latt}
0.076	0.3912(12)	0.393	0.42865(456)
0.07512	0.1737(24)	0.176	0.20623(409)
0.07504	0.1419(17)	0.1426	0.17229(336)

Table 1: Measured masses in the broken phase [9]. The zero-momentum time-slice mass $m_{TS}(0)$ is the physical mass, from the conventional viewpoint. The m_R values, obtained as described in the text, differ slightly by the expected perturbative correction. The m_{latt} values are those obtained by CCCS as giving the best fit to free-propagator form at all except the very lowest momenta.

It is important to note that in the symmetric phase the propagator shows no visible deviation from free-field behaviour; see Fig. 1 of CCCS [9] for $\kappa = 0.074$. All three versions of the “mass” are indistinguishable.

However, the situation is quite different in the broken phase. In Figs. 7, 8, 9 I re-plot CCCS’s propagator data using m_R as the mass in ζ . With this mass ζ has zero slope at $\hat{p}^2 = 0$, by construction. However, ζ then rises with \hat{p}^2 ; quickly at first, then more slowly. The deviation from constancy is highly significant, statistically. Moreover, the deviation from free-propagator behaviour is even larger at $\kappa = 0.07512$ and 0.07504 , closer to κ_c , than it is at $\kappa = 0.076$.

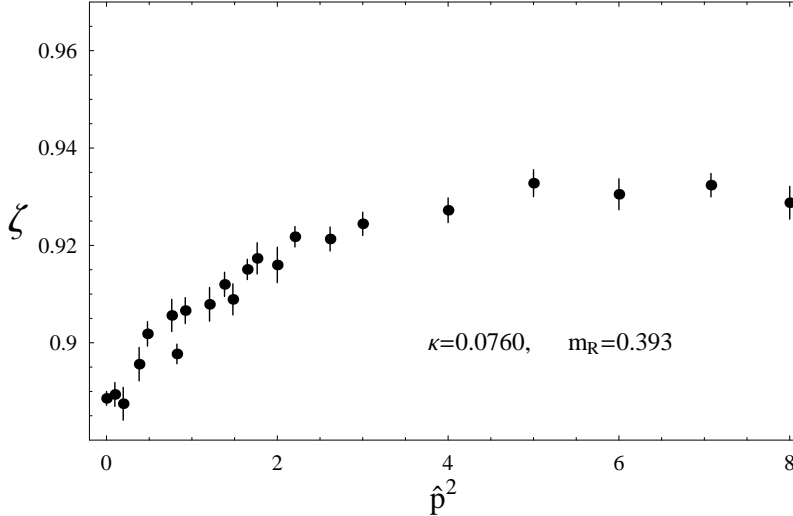


Figure 7: Propagator data for $\kappa = 0.076$ from CCCS plotted as $\zeta \equiv G(\hat{p}^2)(\hat{p}^2 + m^2)$ for a mass $m = m_R = 0.393$. For this mass ζ has zero slope at $\hat{p}^2 = 0$ and its value there is \hat{Z}_R .

While the data sets in Figs. 7, 8, 9 are exactly the same as those shown in Figs. 3, 4, 5 of CCCS [9], the plots have a completely different appearance. This fact is entirely due to the different “m” used in forming ζ , just as one sees in Figs. 6(c),(d) above. In CCCS’s figures, which use m_{latt} , the ζ data points are almost exactly constant, except for the lowest 3 or 4 points, which rise up to a dramatic peak at $\hat{p}^2 = 0$. The peak value, $\zeta(0, m_{\text{latt}})$, is CCCS’s quantity “ Z_ϕ .”

How this situation comes about is illustrated in Fig. 10, which uses a simple fit

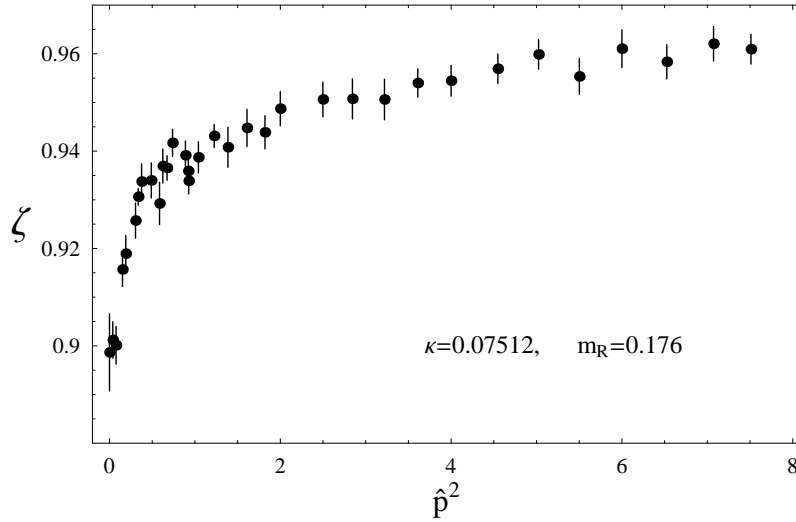


Figure 8: As Figure 7 but for $\kappa = 0.07512$, with $m_R = 0.176$. The scale is exactly the same as Figs. 7 and 9. Notice that the deviation from constancy is even greater than in Fig. 7, even though we are now closer to the continuum limit.

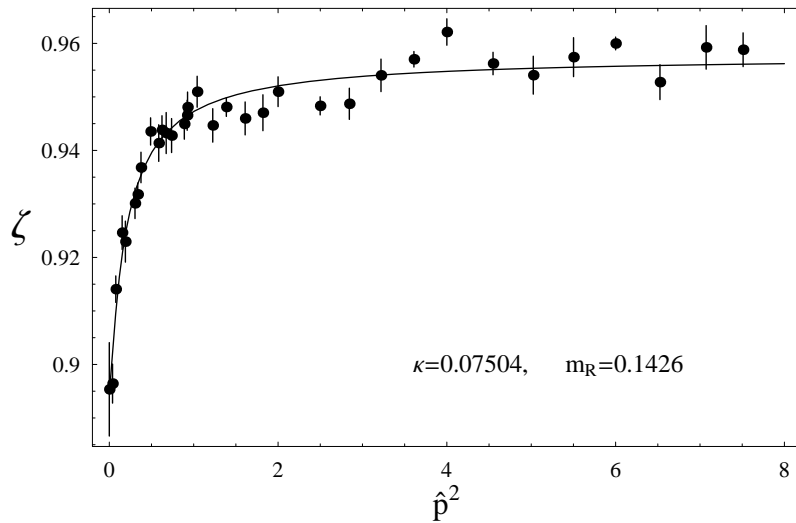


Figure 9: As Figure 7 but for $\kappa = 0.07504$, with $m_R = 0.1426$. The curve represents a simple, empirical fit to the data, to be used in Fig. 10.

to the $\kappa = 0.07504$ data.² The lowest curve corresponds to using $m = m_{TS}(0) \approx m_R$, while the uppermost curve corresponds to using $m = m_{\text{latt}}$, chosen so that the curve is almost exactly flat over the whole range of \hat{p}^2 above, say, 0.1.

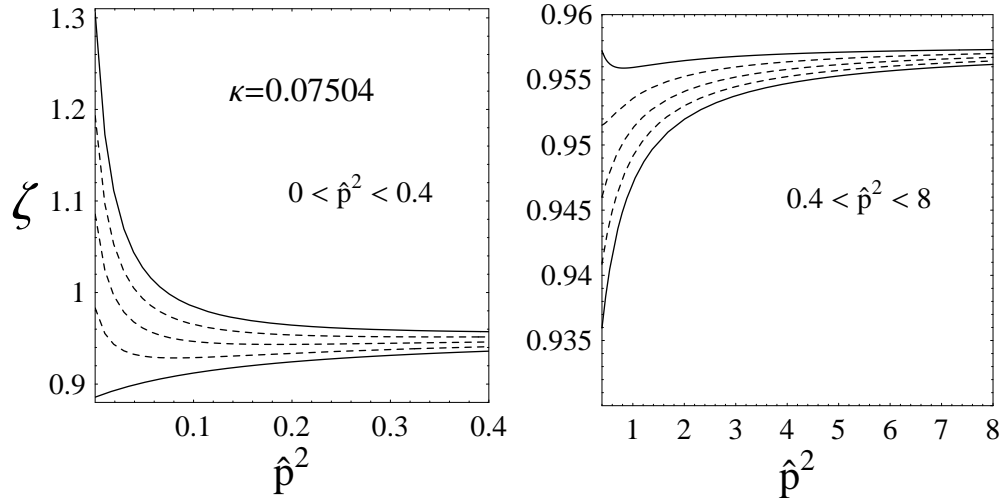


Figure 10: Illustration of the effect of plotting the propagator data as $\zeta \equiv G(\hat{p}^2)(\hat{p}^2 + m^2)$ using different masses m . For clarity, the range of \hat{p}^2 is separated into 0 to 0.4 and 0.4 to 8. The curves use the empirical fit to the $\kappa = 0.07504$ data shown in the previous figure. The lower solid curve represents ζ with $m = m_{TS}(0) = 0.1419$, which differs only slightly from the curve for $m = m_R = 0.1426$ shown in the previous figure. The upper solid curve shows ζ with $m = m_{\text{latt}} = 0.17229$ used in CCCS, Fig. 5. For this mass ζ is essentially constant, as for a free propagator, except for the lowest three data points below $\hat{p}^2 = 0.1$. The dashed curves represent intermediate choices of mass m in equal steps of m between $m_{TS}(0) = 0.1419$ and $m_{\text{latt}} = 0.17229$.

CCCS argue that their data are indicative of a continuum limit in which, with m_{latt} viewed as the physical mass, the propagator tends to free-field form at all finite \hat{p}^2 except for a “spike” in ζ at infinitesimally small \hat{p}^2 . The top of this spike, $Z_\phi = \zeta(0, m_{\text{latt}})$, should diverge to infinity logarithmically in this scenario. Indeed, Z_ϕ grows from 1.05 to 1.31 between $\kappa = 0.076$ and 0.07504. The point I want to

²The fit function corresponds to

$$G(\hat{p}^2) = \frac{A}{\hat{p}^2 + m_{TS}^2(0)} + \frac{B}{\hat{p}^2 + M^2},$$

with parameters $A \approx 0.876$, $B \approx 0.081$ and $M/m_{TS}(0)$ close to 3. This form also fits the propagator data in the other two cases, with quite similar values of A, B and curiously, the best-fit M is again close to $3m_{TS}(0)$.

make here is that the change in viewpoint as to what is the “physical mass” is crucial. Ironically, the “odd” features of the data — which, from the conventional viewpoint are a too-low \hat{Z}_R associated with a distinct *dip* in the ζ plots at low momentum — are, from the CCCS viewpoint, evidence for a logarithmically growing Z_ϕ spike.

6 Non-Ising data

BDWNW also collected some data for the ϕ^4 theory not in the Ising limit, but at $\bar{\lambda} = 0.3$ and 0.6 , where $\bar{\lambda}$ is LW’s parameter that becomes unity in the Ising limit. The other parameters were chosen so that g_R would have a value about 20, for comparison with their Ising data at $\kappa = 0.0751$. Their propagator data at $\bar{\lambda} = 0.3, 0.6$ show no statistically significant deviation from constancy, even if re-plotted using ζ . (However, their data only extend to $\hat{p}^2 = 0.3$ and possibly some effect might show up if one had data at higher momenta.)

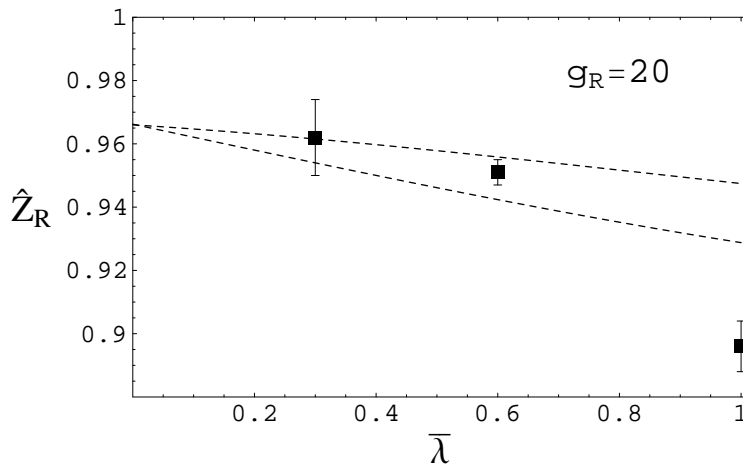


Figure 11: \hat{Z}_R in ϕ^4 theory at $g_R = 20$, as a function of the parameter $\bar{\lambda}$. The region between the two dotted curves represents the prediction of LW(II). The three bold points are the data points from BDWNW, Table 5. A deviation is seen in the Ising case, $\bar{\lambda} = 1$.

Figure 11 plots the BDWNW results for \hat{Z}_R in comparison with the LW expectation, indicated by the region between the two dotted curves. These curves were obtained by finding $\hat{Z}_{\text{crit}} \equiv 2\kappa_c C_2$ from the C_2 ’s of LW(II), Table 1, and the κ_c ’s of LW(I), Table 1, and then applying the perturbative correction, 0.967, relating \hat{Z}_R to \hat{Z}_{crit} at $g_R = 20$. The moral of this plot is that the \hat{Z}_R problem discussed earlier

appears to show up only in the Ising case; i.e., it becomes visible only for $\bar{\lambda}$ above 0.6.

7 Summary and Conclusions

In many respects the RG predictions of LW are impressively successful; they explain a large amount of data over a sizeable range. However, on close examination, there does appear to be a significant problem: The parameters that fit the broken-phase data well (Fig. 1) do not fit the symmetric-phase data for \hat{Z}_R (Fig. 2(a)). Alternatively, parameters that fit the symmetric-phase data well (Fig. 3), and which accord well with LW’s predicted values, do not fit the broken-phase data (Fig. 4). The core of the problem is that the data require a downward step in \hat{Z}_R of 0.07 across the phase transition, whereas the theory predicts a step of only about 0.04. This is a serious concern because it is the proudest boast of the RG method that it can relate the behaviours on each side of the phase transition.

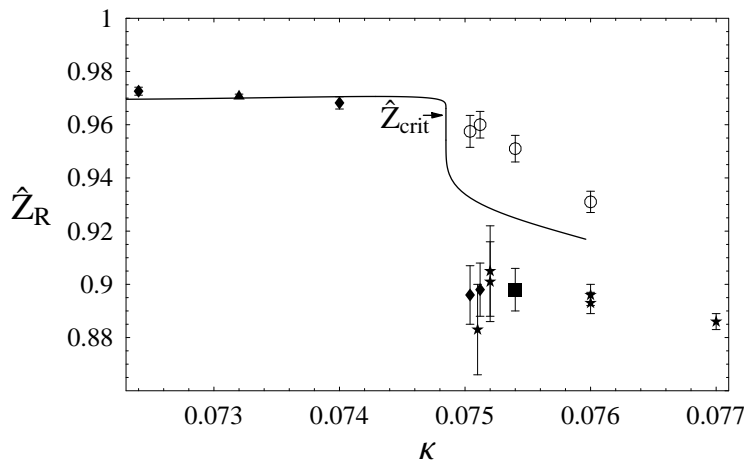


Figure 12: The “step” in \hat{Z}_R across the phase transition, revisited. The solid curve is the RG prediction using the parameters of Figs. 3 and 4 that fit the symmetric-phase data well. The open circles represent “ \hat{Z}_{prop} ” determined from the ζ values of the large- \hat{p}^2 propagator data. I have used some “editorial license” to omit some data points that I consider dubious or uninformative (see discussion in the Appendix).

Figure 12 represents my best summary of the situation, expressed in conventional terms. The RG curve here corresponds to C_i parameters chosen to give a good fit to the *symmetric*-phase data. Relative to this RG prediction, the measured

\hat{Z}_R 's in the broken phase are too low. The open circles correspond to “ Z_{prop} ” determined from the large- \hat{p}^2 behaviour of the propagator data. These points appear to join smoothly to the symmetric-phase points (where \hat{Z}_R and \hat{Z}_{prop} are indistinguishable). In the broken phase, the vertical gap between the open circles and the \hat{Z}_R data points is a measure of the deviation from free-propagator behaviour. Note that this gap *increases* as one approaches κ_c .

Because of the effect illustrated in Fig. 10 these features of the data can be re-interpreted, from CCCS's viewpoint, in terms of a logarithmically growing Z_ϕ . From the conventional viewpoint, one can only say that there is a puzzle that remains to be resolved. My conclusion is that there is strong motivation for collecting more Ising-model lattice data, especially closer to κ_c , on both sides, where the residual uncertainties from higher-twist effects will be even smaller.

Acknowledgements

I am most grateful to Paolo Cea and Leonardo Cosmai for permission to quote some of their new, unpublished data. I thank them and Maurizio Consoli for many discussions. I am also grateful to Anthony Duncan and Ray Willey for helpful discussions about the BDWNW results. This work was supported in part by the Department of Energy under Grant No. DE-FG05-97ER41031.

Appendix: Data

The broken-phase data in Fig. 1 come from various sources. Triangles (\blacktriangle) represent data for χ and v from CCC [7]. Stars (\star) represent data from BDWNW [8] and also an earlier data point from Jansen *et al* [6] at $\kappa = 0.076$. A convenient compilation of these data points can be found in Table 3 of BDWNW [8]. Diamonds (\blacklozenge) represent data at $\kappa = 0.07512$ and 0.07504 for \hat{Z}_R , g_R , and m_R that I have extracted from results of CCCS Ref. [9]. (The CCCS results at 0.076 agree completely with Jansen *et al*.)

The symmetric-phase data in Fig. 2 also come from various sources. Triangles (\blacktriangle) represent data from Montvay, Münster, and Wolff [5]. Stars (\star) represent earlier data from Montvay and Weisz [4]. The diamond (\blacklozenge) at $\kappa = 0.074$ comes from CCCS [9]. The diamond at $\kappa = 0.0724$ represents unpublished data of Cea and Cosmai [10]; see comments below.

In general there appears to be very satisfactory agreement between the data of the various groups. (To avoid clutter I have generally not plotted a data point that completely agrees with, but is less precise than, the equivalent data point from another group.) A few data points, however, deserve comment because superficially they might appear to weaken my case for a large step in \hat{Z}_R .

The BDWNW data point for \hat{Z}_R at $\kappa = 0.0754$ appears high in comparison with the others. I believe that the most likely explanation is an unlucky 2σ statistical fluctuation. I say this (and it implies no criticism of BDWNW) for two reasons: (i) \hat{Z}_R in the region $0.075 < \kappa < 0.076$ is expected to vary slowly and smoothly, so at least one of the BDWNW points must be shifted by more than 1.5σ . Since the other BDWNW points are well corroborated by independent data, the 0.0754 point is the likely culprit. (ii) The 0.0754 data point also seems to lie slightly off the fit curves in the m_R and g_R plots ((e) and (f) in either Fig. 1 or Fig. 4); the hypothesis that the m_R value has a 2σ upward fluctuation would explain away all the discrepancies.

In fact, after having written the previous paragraph, I learned of new data of Cea and Cosmai [10] at the same κ , which indeed yield a smaller mass, $m_R = 0.262(1)$ and a lower $\hat{Z}_R = 0.898(8)$. This result is included in the \hat{Z}_R figures as a square (\blacksquare). (To avoid clutter it has not been included in the m_R plots.)

In the symmetric phase, the $\kappa = 0.0724$ result of Montvay *et al* [5] for \hat{Z}_R appears to be considerably lower than its two neighbouring points, also from Montvay *et al*. The quoted errors are very small, so statistics should not be a factor.

The predicted \hat{Z}_R in this region is almost exactly constant, so the sharp dip implied by the three Montvay *et al* (\blacktriangle) points (see Fig 2(a) or 3(a)), if it were real, would be in serious disagreement with theory. Because of this anomaly I asked Cea and Cosmai to repeat the Monte-Carlo calculation of \hat{Z}_R at the three κ values studied by Montvay *et al*. They kindly did so [10] and found excellent agreement at 0.0710 and 0.0732, but at 0.0724 they found a different result that indeed interpolates smoothly between the neighbouring κ 's. I therefore suspect that there must be some trivial mistake in Montvay *et al*'s 0.0724 point – perhaps in the transcription of the actual computer result to the published paper.

The symmetric-phase data point at $\kappa = 0.074$, closest to the phase transition, is obviously important. The Montvay-Weisz (MW) data point (\blackstar) for m_R comes from the last line of Table 2a of [4] as 0.2125(10) times a factor 1.002 (see last sentence of Sect. 3.1) to convert the physical (or “time-slice”) mass to m_R . This gives 0.2129(10), which agrees very well with CCCS’s result 0.2141(28) (not shown in the figures). The MW result for \hat{Z}_R also comes from the last line of Table 2a of MW, from “ $z = 6.44(10)$ ” converted by a 2κ factor and $(1.002)^2$ (see Eqs. (26), (27) in MW), giving $\hat{Z}_R = 0.957(15)$. This is compatible with the more precise value from CCCS, 0.9682(23) obtained from propagator data. The g_R value from MW comes from remarks in their Sect. 4.2 that a g_R of 24 with a 10 – 15% possible variation would fit their data.

References

- [1] E. Brézin, J. C. Le Guillou, and J. Zinn-Justin, in Vol. 6 of *Phase Transitions and Critical Phenomena*, ed. C. Domb and M. S. Green, Academic Press, London (1976).
- [2] M. Lüscher and P. Weisz, Nucl. Phys. B290 [FS20] (1987) 25.
- [3] M. Lüscher and P. Weisz, Nucl. Phys. B295 [FS21] (1988) 65.
- [4] I. Montvay and P. Weisz, Nucl. Phys. B290 [FS20] (1987) 327.
- [5] I. Montvay, G. Münster, and U. Wolff, Nucl. Phys. B305 [FS23] (1988) 143.
- [6] K. Jansen, I. Montvay, G. Münster, T. Trappenberg, and U. Wolff, Nucl. Phys. B322 (1989) 698.

- [7] P. Cea, M. Consoli, and L. Cosmai, hep-lat/0407024; (see also hep-lat/0501013)
- [8] J. Balog, A. Duncan, R. Willey, F. Niedermayer, and P. Weisz, Nucl. Phys. B714 (2005) 256. (hep-lat/0412015).
- [9] P. Cea, M. Consoli, L. Cosmai, and P. M. Stevenson, Mod. Phys. Lett. A14 (1999) 1673. (hep-lat/9902020).
- [10] Unpublished data from P. Cea and L. Cosmai (private communication).
- [11] A. Agodi, G. Andronico, P. Cea, M. Consoli, L. Cosmai, R. Fiore, and P. M. Stevenson, Mod. Phys. Lett A12 (1997) 1011. (hep-lat/9702407).
- [12] M. Consoli and P. M. Stevenson, Z. Phys. C63 (1994) 427 (hep-ph/9310338); Phys. Lett. B391 (1997) 144 (hep-th/9605122); Intl. J. Mod. Phys. A 15 (2000) 133. (hep-ph/9905427).
- [13] D. Stauffer and J. Adler, Int. J. Mod. Phys. C8 (1997) 263.
- [14] D. S. Gaunt, M. F. Sykes, and S. McKenzie, J. Phys. A12 (1979) 871.
- [15] R. Kenna and C. B. Lang, Nucl. Phys. B393 (1993) 461; Erratum B411 (1994) 340. (hep-lat/9210009).
- [16] C. Vohwinkel and P. Weisz, Nucl. Phys. B374 (1992) 647.